Journal of Materials and Environmental Sciences
ISSN : 2028-2508
CODEN : JMESCN

J. Mater. Environ. Sci., 2018, Volume 9, Issue 10, Page 2919-2925

http://www.jmaterenvironsci.com

New experimental and theoretical studies of two series of tripods based on pyrazole

I. Bouabdallah[1,2*], M. Rahal[3,4], T. Harit[1], I. Zidane[5], R. Touzani[6], A. El Hajbi[3], F. Malek[1]

1. Laboratoire de Chimie Organique, Macromoléculaire et Produits Naturels, URAC25, Faculté des Sciences, Université Mohammed I^er, BP 524, 60 000 Oujda, Maroc.
2. Équipe de Recherche en Chimie et Didactique, Centre Régional des Métiers de l'Éducation et de la Formation, Oujda, Maroc.
3. Laboratoire de Chimie Physique, Faculté des Sciences, Université Chouaib Doukkali, 24000 El Jadida, Maroc.
4. Centre Régional des Métiers de l'Éducation et de la Formation, Région Laayoune Boujdour Saguia El Hamra, Maroc.
5. Faculté des Sciences, Université Ibn Tofail – Kénitra, Maroc.
6. Faculté Pluridisciplinaire, Université Mohammed I^er, 62700 Selouane, Nador, Maroc.

Received 24 May 2017,
Revised 01 Aug 2017,
Accepted 10 Aug 2017

Keywords

- ✓ Comparison;
- ✓ Isomer;
- ✓ Tripod;
- ✓ Pyrazole.

I. Bouabdallah
bouabib2002@yahoo.fr
+212536684705

Abstract

New comparative experimental and theoretical studies of two isomeric series of tripods based on pyrazole rings were investigated. Tripods were characterized by the presence of two types of connecting junctions N-C-N (**1**, **3**) and N-C-C (**2**, **4**). Melting points, IR, NMR and MS spectra of ligands **1**-**4** were examined. All geometrical parameters were computed using density functional theory method (B3LYP) with 6-311+G (2d,p) as basis set. The nature of junctions between the aniline N-atom and the pyrazole rings influence considerably the melting points, chemical shifts, fragmentation pattern, bond angles and orientations between pyrazolic rings. However, the junction modes produce small variations on the bond lengths in side arms.

1. Introduction

Pyrazolic compounds represent a large source for various applications with industrial, biological and medical purposes [1–6]. Tripod ligands based on the pyrazole moieties are a very popular class of organic structures, assembling sp^2 and sp^3 hybridized nitrogen atoms. The electronic doublets of three donor sites are organized according to a pyramidal form for complexing metal leading to a wide range of application fields in chemistry. According to the junction, bonding the pyrazolic ring to the side arm, two isomeric series of tripods can be distinguished. The first one is characterized by the presence of two N-C-N junctions, and can be prepared from reaction between 1-(hydroxymethyl)-3,5-dimethylpyrazole (**I**) and primary amines [7]. The substitution of **I** by 3-chloromethyl-1,5-dimethylpyrazole (**II**) led to second series presenting two N-C-C junctions [8,9]. As reported in the literature, these junction differences between the two series of isomers affected considerably the molecular geometry [8], inhibition properties of the ligands towards corrosion [10], cytotoxic activities [11], liquid-liquid extraction [12] and catalytic properties [13]. However, some isomeric tripods exhibit similar properties [13]. As part of our laboratory research program, we compare in this paper the melting points, IR, NMR and MS spectra and the geometrical parameters of the two isomeric series of tripods based on the pyrazole rings in order to provide probable explanations for differences and similarities previously cited. To perform this study, we have selected as model four compounds synthesized as show in scheme 1: N,N-bis(3,5-dimethyl-pyrazol-1-ylmethyl)-N,N-dimethyl-p-phenylenediamine **1** [14] ; N,N-bis[(1,5-di-methylpyrazol-3-yl)meth-yl]-

N,N-dimethyl-p-phenylenediamine **2** ; N,N-bis(3,5-dimethyl-pyrazol-1-ylmethyl)benzylamine **3** [15] and N,N-bis[(1,5-dimethylpyrazol-3-yl)methyl]benzylamine **4** [9]. Thus, the density functional theory (DFT) method has been used to determine the geometrical parameters [16].

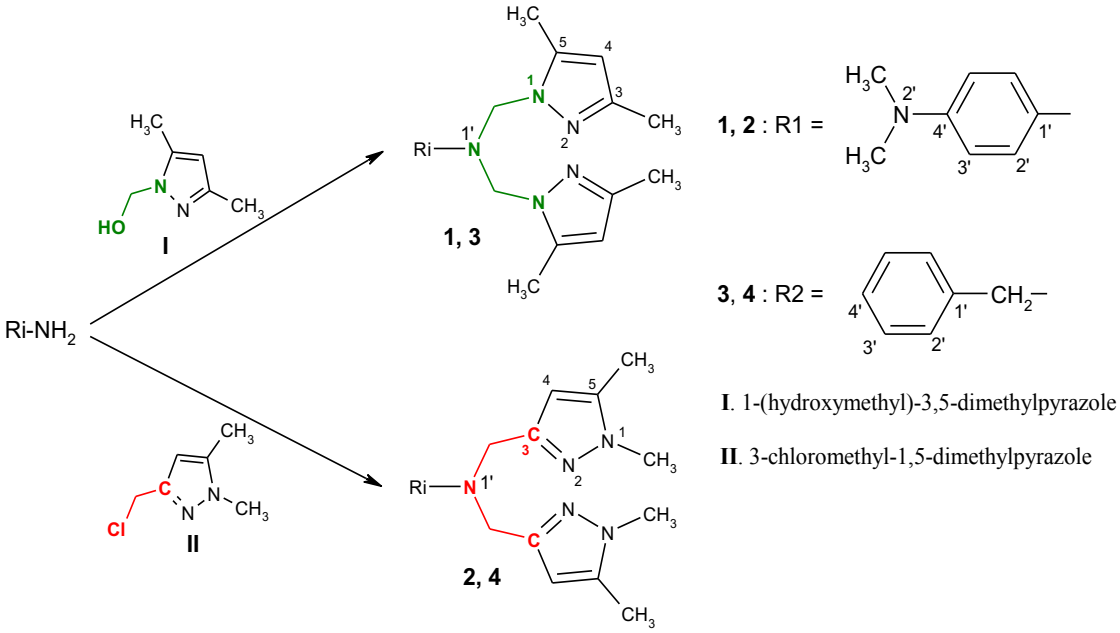

Scheme 1: Synthesis of compounds **1-4**

2. Experimental and computational details

2.1. Experimental details

Apparatus: Melting points uncorrected were determined on BUCHI 510 MP apparatus. The IR spectra were taken with potassium bromide discs on PERKIN ELMER 1310 spectrometer. NMR spectra were recorded on a BRUKER 300 (operating at 300.13 MHz for ^{1}H, 75.47 MHz for^{13}C) spectrometer. Chemical shifts are listed in ppm and are reported relative to tetramethylsilane, residual solvent peaks being used as internal standard. Mass spectra were obtained on a VG7070E spectrometer, using electron ionization.

Synthesis: Compound **2** was synthesized by refluxing a mixture of N,N-dimethyl-para-phenylenediamine (0.680 g, 5mmol), 3-chloromethyl-1,5-dimethylpyrazole (1.44 g, 10 mmol) and sodium carbonate (4.24 g, 40 mmol) in acetonitrile (30 mL) for three hours. The solvent was removed at reduced pressure and the residue was purified to give **2** as a black product. Yield : (915 mg , 52 %); R_f : 0,3 (alumina / CH_2Cl_2 + EtOH: 90/10); m. p. 110 - 112°C (CH_2Cl_2); ^{1}H-NMR ($CDCl_3$, δ, ppm) : 2.20 (s, 6 H, C5-CH_3), 3.06 (s, 6 H, N($C\underline{H}_3$)$_2$), 3.70 (s, 6 H, N-$C\underline{H}_3$), 4.37 (s, 4 H, N-$C\underline{H}_2$-pz), 5.84 (s, 2 H, C4-$\underline{H}$), 6.93 (m, 2 H, H3'), 7,41 (m, 2 H, H2'), ^{13}C-NMR ($CDCl_3$, δ, ppm) : 11.37 (C5-$\underline{C}H_3$), 36.15 (N-$\underline{C}H_3$), 53.74 (N($\underline{C}H_3$)$_2$), 65.73 (N-$\underline{C}H_2$-C), 105.15 (C4), 117.88 (C2'), 139.33 (C1'), 139.51 (C5), 132.42 (C3'), 152.06 (C3), 152.96 (C4'); IR (KBr, cm^{-1}) : 3040 ($\nu_{C\text{-}H,\ arm.}$), 2945 ($\nu_{C\text{-}H,\ CH3}$), 2812 ($\nu_{C\text{-}H,\ CH2}$), 2800 ($\nu_{C\text{-}H,\ N\text{-}CH3}$), 1600 ($\nu_{C=N}$), 1494 ($\nu_{C=C}$), 1370 ($\delta_{C\text{-}N}$), 1200, 1140, 989, 810 ($\delta_{=C\text{-}H}$) ; MS (EI), m/z: 352, 301, 243, 227, 147, 121, 110, 95, 77, 56, 36.

2.2 *Computational details*

All of the geometry optimizations were performed by the density functional theory (DFT, B3LYP) which were implemented in the Gaussian03W program [16-18]. The 6-311+G(2d,p) basis set was used for all calculations and the geometries were determined without any symmetry constraints. 6-311+G(2d,p) is a split-valence triple-zeta basis set arising from the group of John Pople completed by diffuse functions on heavy atoms (+), 2 d-type Cartesian Gaussians polarization functions on heavy atoms (2d) and p-type polarization functions on hydrogen atoms (p) . 6 represents the number of primitive Gaussians comprising each core atomic orbital basis function.3,1,1 indicate that the valence orbitals are composed of three basis functions each, the first one composed of a linear combination of *3* primitive Gaussian functions, the two others (1,1) composed of a linear combination of *1* primitive Gaussian functions. Harmonic frequencies of every structure were calculated in order to ensure that the optimized geometry really corresponded to a true local minimum energy on the potential energy surface. GaussView 5.0.8 visualisation program [19] has been used to develop the molecular structure.

3. Resulats and Discussion

3.1. Synthesis

Compounds (**1**, **3**) and (**2**, **4**) belong respectively to the first (N-C-N) and second (N-C-C) series. The structures of isomers **1** and **2**, and **3** and **4** differ in the junction mode between the nitrogen center and the pyrazolic rings. Tripods **1**, **3** and **4** have been already described and characterized [9,14,15]. Ligand **2** was prepared by condensation of one equivalent of N,N-dimethyl-para-phenylenediamine with two equivalents of **II** in refluxing acetonitrile for three hours, using sodium carbonate as base. The structure of **2** has been determined by IR, MS, NMR (^{1}H, ^{13}C) spectroscopy.

3.2. Melting points

Analysis of melting points reported in Table 1, shows the following order **2** > **1** > **3.** Ligand **4** has a viscous appearance. So, the benzyl group induces a decrease of melting point and a variation is $\Delta m.p._{1\rightarrow3}$ = -18°C. This result indicates that the strength of the force of attraction between the particles in **1** are very intense than those in **3**. Also, N-C-C junction mode leads to increased melting points ($\Delta m.p._{1\rightarrow2}$ = 22°C). These differences indicate that the two isomers must have different structural arrangements of atoms or configurations. Thus, probable stronger intermolecular interactions in **2** having N-C-C junctions result higher melting point. This property agrees with the similar reported isomers [8].

Table 1: Comparison between pairs (**1**,**2**) and (**3**,**4**)

	Entry	m.p. (ºC)	δ (-N(C$\underline{H}_3$)$_2$/(C$\underline{H}_3$)$_2$)	δ (C$\underline{H}$3')	δ (C$\underline{H}$2')	δ (ph-C$\underline{H}_2$/C$\underline{H}_2$-N)	δ (N-C$\underline{H}_2$-pz)	δ (C5-C$\underline{H}_3$)
m.p. and ^{1}H NMR spectra	**1**	88-90	2.83/41.22	6.53	6.68	--	5.30	1.85
	2	110-112	3.06/53.74	6.93	7.41	--	4.37	2.20
	3	71-72	--	7.23	7.14	3.66/52.83	4.90	1.96
	4	Viscous	--	7.23	7.11	3.52/57.39	4.26	2.14
Mass spectra	**1**	352 (39.2%),[a] 243 (12.0%), 215 (14.7%), 148 (100.0%),[b] 147 (50.0%), 109 (79.9%), 96 (22.1%), 77 (5.7%), 54 (4.0%), 42 (11.5%)						
	2	352 (43.5%),[a] 243 (100.0%),[b] 227 (10.4%), 147 (6.2%), 121 (15.9 %), 121 (15.9%), 109 (43.3%), 110 (61.0%), 95 (9.7%), 77 (3.82 %), 56 (11.3%), 36(12.4%).						
	3	323 (0.1%),[a] 228 (75.7%), 185 (16.3%), 173 (3.5%), 150 (3.6%), 136 (52.6%), 109 (100.0%),[b] 91 (58.0%), 80 (4.5%), 68 (11.4%), 54 (4.8%), 42 (36.2%).						
	4	323 (0.8%),[a] 279 (0.2%), 248 (1.0%), 232 (85.0%), 214 (91.1%), 197 (4.8%), 149 (3.3%), 124 (3.8%), 109 (100.0%),[b] 91(86.7%), 82 (5.3%), 56 (25.9%), 42 (17.9%)						

[b] Molecular ion peak, [b]Base peak

3.3. IR, NMR and MS analysis

Direct and simple analysis of the literature IR spectra of compounds **1, 3, 4** and the recorded spectrum for **2** shows the absence of N-H vibrations, characteristic of amines. Bands located between 2900 and 3060 cm^{-1} are assigned to $\nu_{C\text{-}H.}$ So, investigations of the effects of junction mode and side arm on the infrared vibrational spectra are not effective.

Results (Table 1) show that the ^{1}H NMR spectrum of **1** revealed signals at 2.83 and 5.30 ppm corresponding respectively to protons N(C$\underline{H}_3$)$_2$ and N-C$\underline{H}_2$-N. Whereas the chemical shifts for protons in isomer **2** are 3.06 (N(C$\underline{H}_3$)$_2$) and 4.37 (N-C$\underline{H}_2$-C) ppm. So, substitution of N-C-N junction by N-C-C one in **1** induced a decrease in deshielding of protons H2' (0.73 ppm), H3' (0.40 ppm) and N(C$\underline{H}_3$)$_2$ (0.23 ppm). However, this effect was not conserved in **3** and **4**, and the protons are shielded of 0.14 (ph-C$\underline{H}_2$-N) and 0.03 (H2') ppm. Also, ^{13}C-NMR analysis of chemical shifts attributed to the carbons N(C$\underline{H}_3$)$_2$, C4', C3', C2' and C1'showed a significant increase effects ranging 2.95 - 11.52 ppm through **1** to **2**. But, an opposite change was found between **3** and **4**. These results clarified the influence of junction mode in both ^{1}H and ^{13}C chemical shifts.

Comparison of the EIMS of **1** and its isomer **2**, the spectra of **3** and **4,** shows that the character of fragmentation depends on the junctions and side arms. The MS data for all isomers showed that the molecular ions peaks are only visible for pair (**1**,**2**) and they appeared at m/z 352, in good agreement with their molecular formula $C_{20}H_{28}N_6$. But, for pair (**3**,**4**) molecular ion peaks are not significant because the ions are unstable and fragments give similar characteristics. It is noted that the parent ion fragmentation gives two major peaks. In all ligands, the peak located at m/z 109 corresponds to 3,5-dimethylpyrazol-1-ylmethyl or 1,5-dimethyl-pyrazol-3-ylmethyl arms, and a peak at m/z 91 in **3** and **4** is attributed to benzyl group. This phenomenon is due to the presence of methylene group between benzene ring and aminic nitrogen, excluding any conjugation with free electron of the aminic nitrogen, leading to high molecular ion stability.

By contrast, for isomers **1** and **2** the base peaks are different and inducing fragmentations follows distinct routes as represented in scheme 2. MS of **1** revealed two possibilities of decompositions, leaded to variable abundance peaks. The cleavage according to "A", leads to the ions at m/z 95 (16.5%) and m/z 257 (6.1%). Fragmentation of the latter ion results the ion m/z 161 with average abundance of 32%. While, the fragmentation according to "B" results two ions, one has a high relative abundance at m/z 109 (79.9%) and other at m/z 243 (12%). This instable ion leads to the base peak ion at m/z 148 (100%). Therefore the bond between carbon and pyrazole is more stable than the sp^3 nitrogen-carbon junction. This property gives the greater flexibility in **1**. For ligand **2**, according to the "A" fragmentation, two peaks with low abundances, at m/z 95 and 257 were generated. While the cleavage according to the ‘‘B’’ generates ion corresponding to base peak at m/z 243 (100%) and ion at m/z 109 (43.3%). The fragmentation according to the “C” of the most abundant molecular ion leads to the ion at m/z 148 with low abundance (2.3%). This shows that the fragmentation according to the "A" and "C" are less probable than these according to the "B". Therefore the bond between the carbon and pyrazole ring is very stable towards the junction between the aminic nitrogen and carbon, in good agreement with the literature [7, 8]. Therefore, in these isomers C-Pyrazol bond is more stable than N-C.

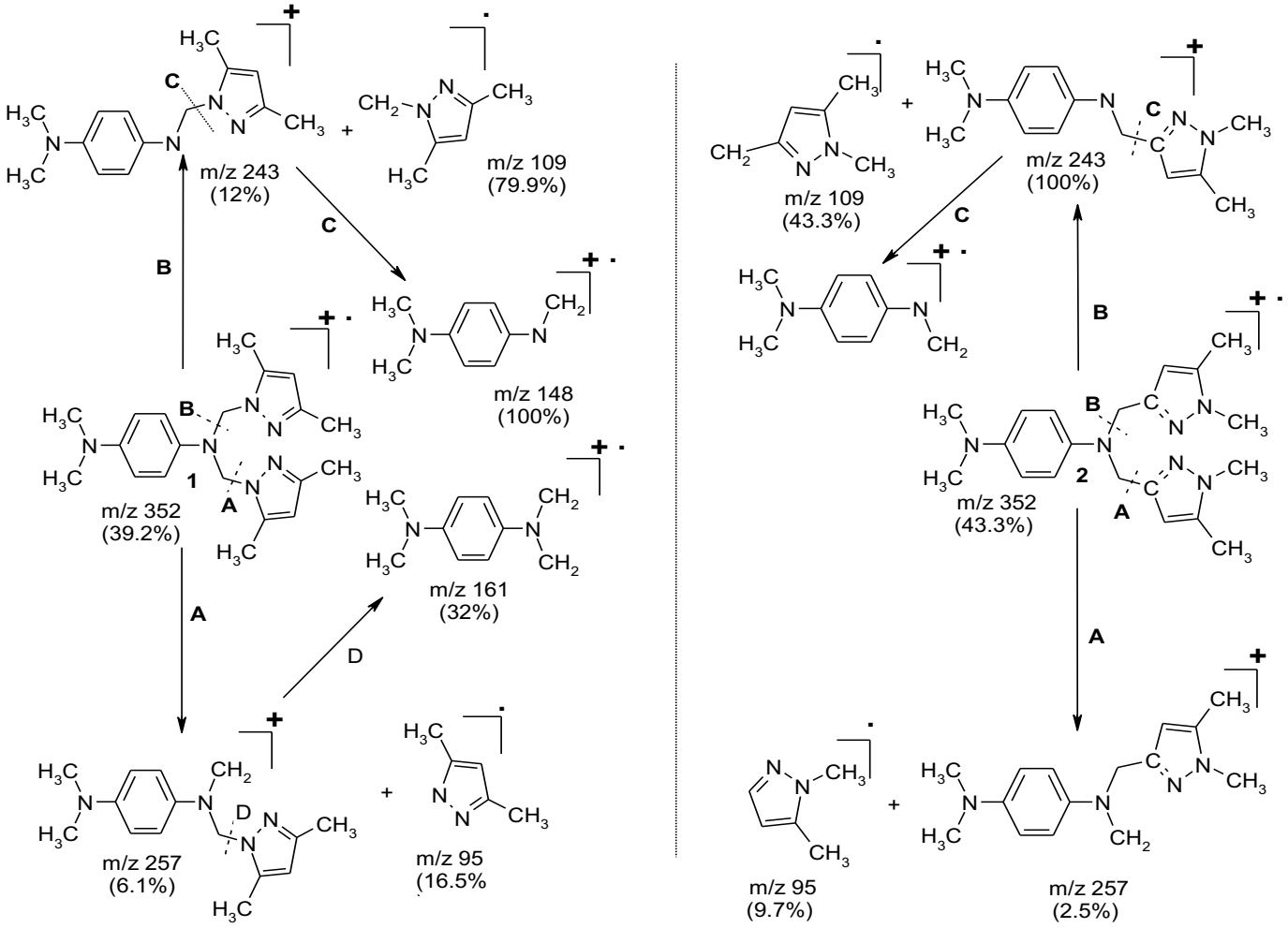

Scheme 2: EIMS spectral fragmentation mechanism of compounds **1** and **2**

3.4. Geometrical parameters

To simplify the analysis of junction mode and side arm effects on the molecular geometry, we restricted attention to three representative properties such as bond lengths, bond angles and dihedral angles. Currently, to best of our knowledge exact experimental crystal structures of the investigated compounds have not yet been reported. In this discussion, we examine the optimized structures (Figure 1) obtained by B3LYP/6-311++G(2d,p) method which is known to be an excellent computational choice both to calculate geometric data [20]. Selected calculated geometric parameters are presented in Table 2. Hence, the crystal data of closely

related molecules is compared with that of the studied compounds [8,21,22]. Indeed, the N1-N2 bond lengths are calculated as 1.36326/1.35936 and 1.36382 /1.35924Å respectively for **1** and **3** are slightly longer than the similar reported value of 1.353Å [21]. Also, the literature C4-C5 bond lengths of 1.360/1.359Å are shorter than those calculated for compounds with N-C-N junctions (1.37847/1.37842-1.37820/1.37851Å) [21]. Thus, the differences between experimental and theoretical bond lengths may be attributed to intermolecular hydrogen bonding advantaged with carboxyl groups. As well, the isolated molecule is considered in gas phase in theoretical calculation, whereas many packed molecules are treated in condensed phase during the experimental measurement.

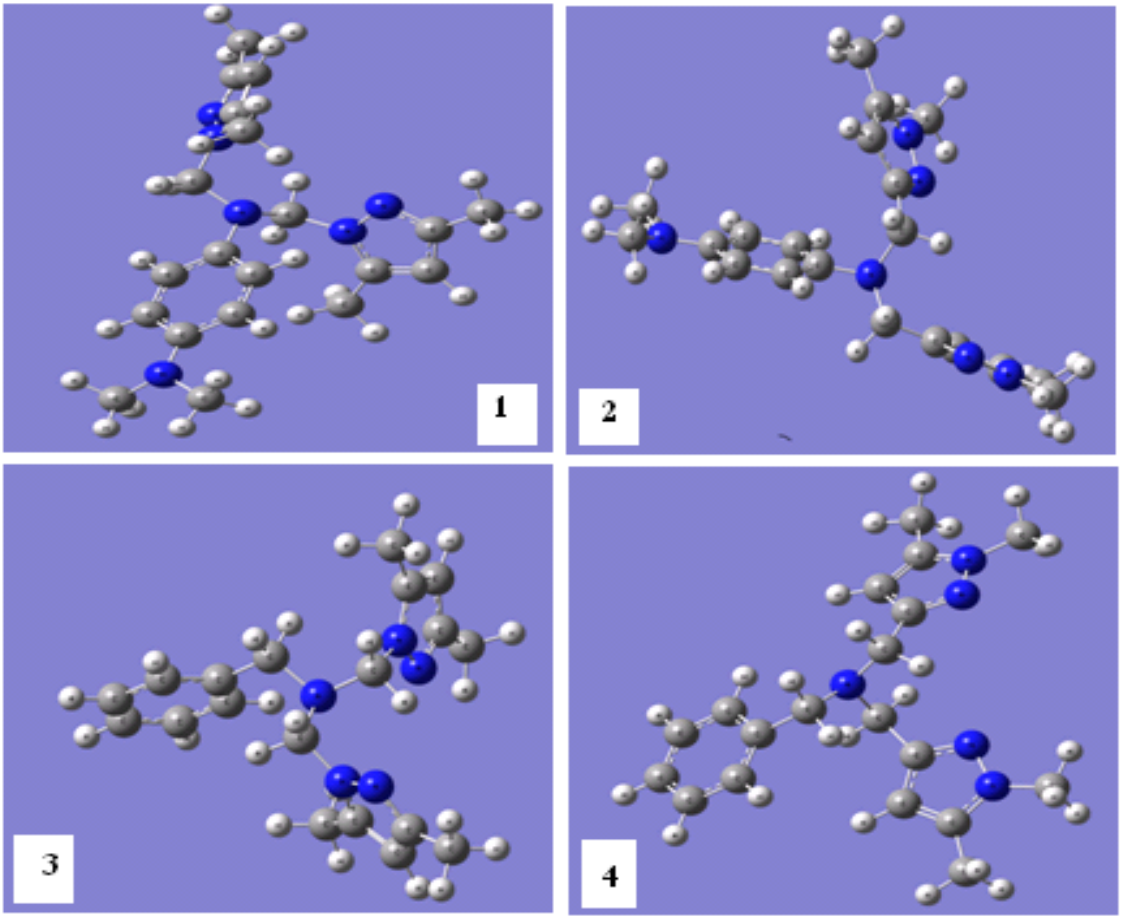

Figure 1: Optimized structures of **1-4** measurements

Table 2: Selected calculated (B3LYP/6-311+G(2d,p)) geometric parameters

Junctions	N-C-N			N-C-C		
	Bond length (Å)					
Compounds	**1**	**3**	Experimental [22]	**2**	**4**	Experimental [8]
N1-N2	1.363/1.359	1.364/1.359	1.370/1.379	1.355/1.354	1.355/1.354	1.362/1.364
C4-C5	1.379/1.378	1.378/1.379	1.377/1.390	1.380/1.380	1.381/1.380	1.376/1.376
C1'-N1'	1.435	--	1.447	1.435	--	1.407
N2'-C4'	1.391	--	--	1.397	--	--
H_3C-N2'	1.453/1.453	--	--	1.452/1.452	--	1.451/1.451
C1'-CH_2	--	1.5134	--	--	1.5171	--
PhCH_2-N1'	--	1.46707	--	--	1.461	--
C1'-C2'	1.396	1.394	1.396	1.395	1.396	1.395
	Bond angle (°)					
N1-N2-C3	105.439/105.297	105.316/105.501	105.8/104.8	105.248/105.217	105.292/105.437	104.65/104.57
C5-N1-N2	112.150/112.210	112.177/112.051	112.0/113.1	112.463/112.212	112.408/112.279	112.72/112.42
C5-C4-C3	105.889/105.733	105.914/105.734	106.6/106.5	105.667/105.393	105.686/105.453	106.38/106.17
CH_2-N1'-CH_2	112.802	112.172	114.1	111.20	113.498	116.45
CH_3-N2'-CH_3	116.698	--	--	116.153	--	--
C1'-CH_2-N1'	--	113.473	--	--	113.766	--
	Dihedral angle (°)					
Pz1/Pz2	64.08	67.56	87.88	38.77	33.00	7.71
Pz1/Ph ; Pz2/Ph	79.60 ; 80.35	60.22 ; 60.72	72.05 ; 50.40	57.39 ; 13.00	21.68 ; 26.22	84.66 ; 79.77

The analysis of bond length changes induced by the mode of junction produces small variations of bond distances in R substituents. Computed C1'-N1', N2'-C4' and H_3C-N2' bond lengths are identical for isomers **1** and **2**. We noticed in **1** that the C1'-N1' bond distance of 1.435 Å is larger than those reported for aniline (1.400 Å [20], 1.398 Å [21]), and is smaller than this determinated for N-C-N bis-tripode of 1.447 Å [22]. The explanation makes use of the idea that the size of substituent influences the bond length and the lone pair of electrons on the nitrogen of aniline are conjugated to the π-electrons of the aromatic ring, the distance N-C becomes shorter and the hybridation of N becomes closer to sp^2**.**

The C1'-C2' bond lengths ranging between 1.394 Å and 1.396 Å compare well with the experimental values [8,22]. Hence, the effect of junctions on the bond lengths in this moiety seems very low.

Besides, internal angles of the pyrazole rings N1-N2-C3 are smaller than C5-N1-N2, which are in good agreement with Botani and Bovio rules [23]. In tripods **1** and **3** the bond angles N1-N2-C3, C5-C4-C3 are larger than that calculated for **2** and **4**. Analysis of CH_2-N1'-CH_2 bond angles, demonstrates different effects of Ri substituents for two series of compounds. Indeed, the CH_2-N1'-CH_2 bond angles of 112.802° in **1** and of 112.172° in **3** are smaller than the experimental value of 116.8° [21]. So, the benzyl group involves a reduction of 0.627° for tripods with N-C-N junctions and an increase of 2.298° for the second series. Also, the CH_3-N2'-CH_3 bond angles of 116.698° and 116.153° respectively for **1** and **2** are larger than the H-N-H bond angle of 111.5 reported for aniline [20]. These results are due to interactions between the substituents linked to the aniline nitrogen. And when the steric strain increases, the value of the angles around the N is greater. Comparison between experimental angle values [8,22] allows to deduct that interactions involved by 1,5-dimethylpyrazol-3-ylmethyl arms are more intense than those due to 3,5-dimethylpyrazol-1-ylmethyl moieties. This rule provides an explanation of results obtained for **3** and **4**, but not sufficient for **1** and **2**.

Furthermore, the notable influence on the molecular geometry is that obtained for the conformations of isomers. Indeed, the dihedral angles between the two pyrazole rings in pair (**1**,**3**) are higher than those obtained in their homologous (**2**,**4**). These results are in good agreement with the experimental data. The orientations of pyrazoles towards benzene nucleus are different in **2** and **4** with dihedral angles of 57.39/13.00° and 26.22/21.68° respectively, in contrast to other tripods where the dihedral angles are similar. In this case, the N-C-C junctions allow changing the arrangement of the planes of pyrazole and benzene rings. We noticed that this effect is very important when the aminic nitrogen is directly linked to benzene.

Conclusions

A combined experimental and density functional theory studies of two isomeric series of tripods based on pyrazole were investigated. Ligands are characterized by the presence of two different types of junctions (N-C-N, N-C-C). The presented results may have potential relevance for understanding the physico-chemical and biological properties of these isomers. Experimental results lead to conclude that by introducing various junctions and moieties, melting points, NMR properties and MS fragmentation modes change. Also, geometrical properties are influenced by two factors. The greatest variations are those obtained for the conformations of isomers described by the bond angles and the orientations between aromatic rings. However, the variations induced by the junction mode on the bond lengths in side arms seem very low.

References

1. Blackburn N.J., Strange R.W., Farooq A., Haka M.S., Karlin K.D., *J. Am. Chem. Soc.* 110 (1988) 4263.
2. Karlin K.D., Ghosh P., Cruse R.W., Farooq A., Gultneh Y., Jacobson R.R, Blackburn N.J., Strange R.W., Zubieta J., *J. Am. Chem. Soc.* 110 (1988) 6769.
3. Kitajima N., Koda T., Haschimoto S., Kitagawa T., Morooka Y., *J. Am. Chem. Soc.* 113 (1991) 5664.
4. Petrova M.A., Kurteva V.B., Lubenov L.A., *Ind. Eng. Chem. Res.* 50 (2011) 12170.
5. Schmidt A., Dreger A., *Curr. Org. Chem.* 15 (2011) 1423.
6. Dias D., Pacheco B.S., Cunico W., Pizzuti L., Pereira C.M.P., *Mini. Rev. Med. Chem.* 14 (2014) 1078.
7. Driessen W.L., *J. Royal Netherlands Chem. Soc.* 101 (1982) 441.
8. Bouabdallah I., Ramdani A., Zidane I., Touzani R., Eddike D., Radi S., Haidoux A., *J. Chem. Res.* April (2005) 242.
9. Bouabdallah I., Touzani R., Zidane I., Ramdani A., *Cat. Comm.* 8 (2007) 707.
10. Dafali A., Hammouti B., Touzani R., Kertit S., Ramdani A., El Kacemi K., *Anti. Corros. Method. Mater.* 49 (2002) 96.

11. Bouabdallah I., Ait M'Barek L., Zyad A., Ramdani A., Zidane I., Melhaoui A., *Nat. Prod. Res.* 20 (2006) 1024.
12. Bouabdallah I., Zidane I., Touzani R., Hacht B., Ramdani A., *Arkivoc*, xi (2006) 59.
13. Bouabdallah I., Touzani R., Zidane I., Ramdani A., *J. Iran. Chem. Soc.* 4 (2007) 299.
14. Bouabdallah, I.; Ramdani, A.; Zidane, I. ; Touzani, R. *Molbank*, 2005, M 398.
15. Malachowski M.R., Davidson M.G., *Inorg. Chim. Acta* 162 (1989) 199.
16. Becke A.D., *Phys. Rev.* A38 (1988) 3098.
17. Parr R.G., Wang W., Density-Functional Theory of Atoms and Molecules; Oxford University Press: New York, 1994.
18. Frisch M.J., et al. Gaussian 03, Revision C.02, Gaussian Inc., Pittsburgh, PA, 2003.
19. Keith T., Millam J., GaussView, Version 5, Roy Dennington, Semichem Inc., Shawnee Mission, KS, 2009.
20. Gomes J.R.B., Ribeiro Da Silva M.A.V., *Int. J. Quantum. Chem.* 101 (2005) 860.
21. Daoudi M., Ben Larbi N., Benjelloun D., Kerbal A., Launay J.P., Bonvoisin J., Jaud J., Mimouni M., Ben-Hadda T., *Molecules* 7 (2002) 690.
22. Daoudi M., Ben Larbi N., Benjelloun D., Kerbal A., Launay J.P., Bonvoisin J., Jaud J., Mimouni M., Ben-Hadda T., *Molecules* 8 (2003) 269.
23. Bonati F., Bovio B., *J. Cryst. Spectrosc. Res.* 20 (1990) 233.

(2018) ; http://www.jmaterenvironsci.com